Stem Cell Reports, Volume *10*

Supplemental Information

Combined Loss of JMJD1A and JMJD1B Reveals Critical Roles for H3K9 Demethylation in the Maintenance of Embryonic Stem Cells and Early Embryogenesis

Shunsuke Kuroki, Yuji Nakai, Ryo Maeda, Naoki Okashita, Mika Akiyoshi, Yutaro Yamaguchi, Satsuki Kitano, Hitoshi Miyachi, Ryuichiro Nakato, Kenji Ichiyanagi, Katsuhiko Shirahige, Hiroshi Kimura, Yoichi Shinkai, and Makoto Tachibana

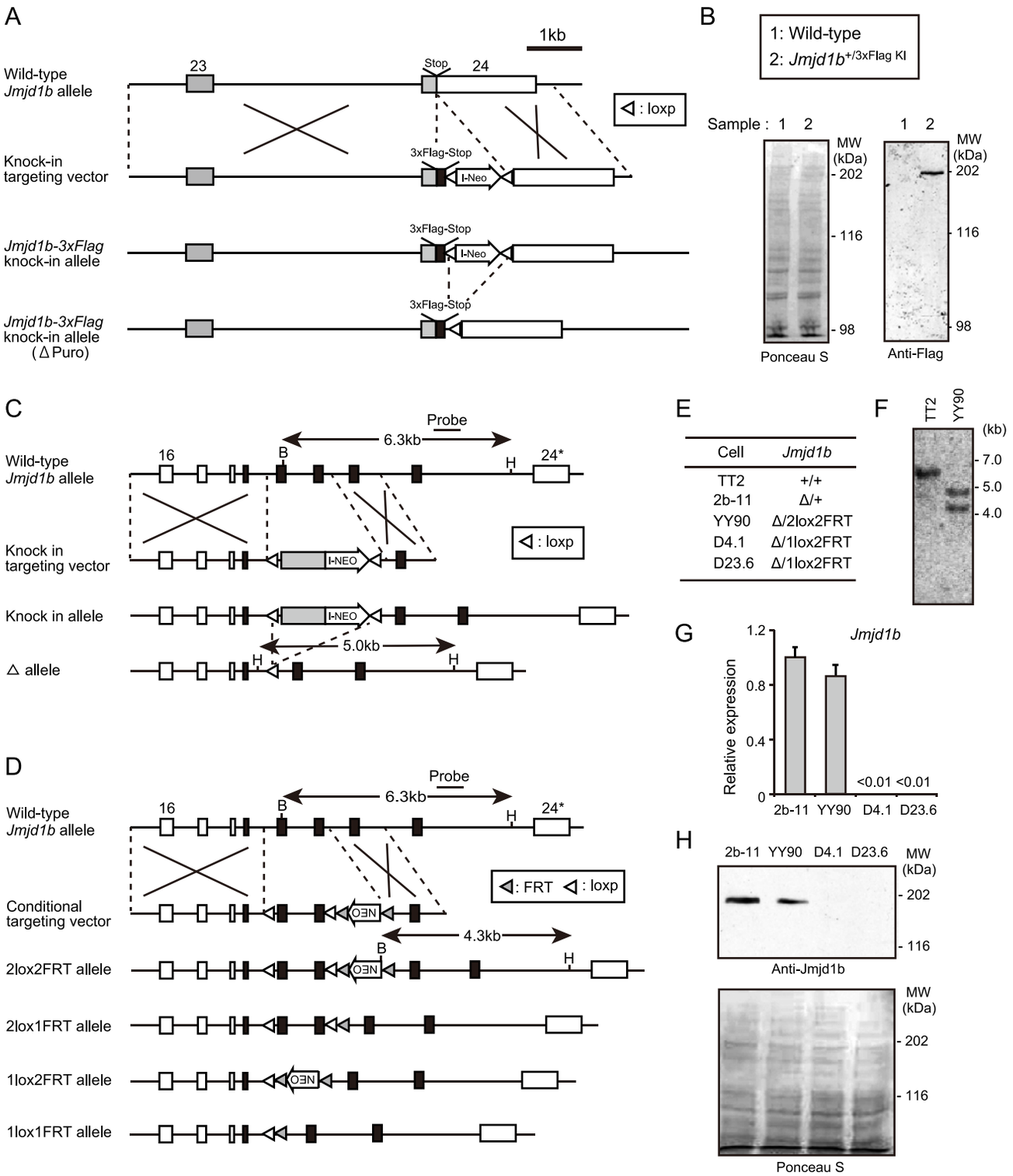

Figure S1. Generation of *Jmjd1b*$^{\text{Flag-KI}}$ Mouse and *Jmjd1b*-Deficient Mouse, Related to Figures 1, 2, and 5.
(A) Targeting strategy for generating *Jmjd1b*$^{\text{Flag-KI}}$ allele. Grey box indicates the coding region of *Jmjd1b*. The knock-in targeting vector involves DNA sequences encoding a triple Flag epitope tag and IRES-Neo, which are inserted at the 5' end of the termination codon in JMJD1B. (B) Immunoblot analysis of *Jmjd1b*$^{+/\text{Flag-KI}}$ ES cells. Whole cell extracts were prepared from the indicated ES cells, separated by SDS-PAGE, and then immunoblotted with anti-FLAG antibody. (C, D) Targeting strategy for generation of *Jmjd1b*$^{\Delta}$ allele (C) and *Jmjd1b*-conditional mutant allele (D). Grey box indicates the protein-coding region of *Jmjd1b* cDNA corresponding to exons 20-24. The targeting vectors were constructed by BAC recombineering technique using a BAC clone RP23-184N15. (E) List of established ES cell lines and their genotypes. (F) Southern blot analysis of wild-type and *Jmjd1b*$^{\Delta/2\text{lox2FRT}}$ ES cells. Genomic DNA was digested with *Hind*III and *Bam*HI, transferred to nylon membrane, and hybridized with a probe as shown in C and D. (G) Expression levels of *Jmjd1b* in the indicated cells were determined by quantitative RT-PCR analysis. Data were normalized to the expression levels of *Gapdh*. Data are presented as mean ± SD (n=3 independent experiments). (H) Whole cell extracts of the indicated cells were separated and immunoblotted with anti-JMJD1B antibodies. Pouceau S staining was used for confirmation of equal protein loading.

A

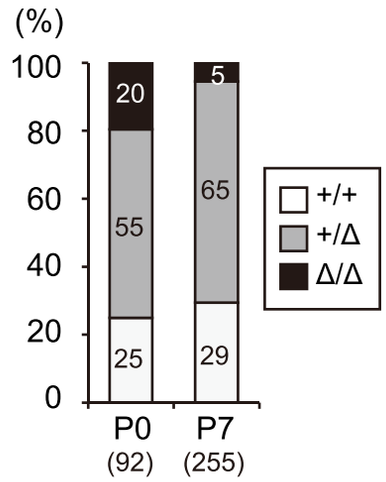

B

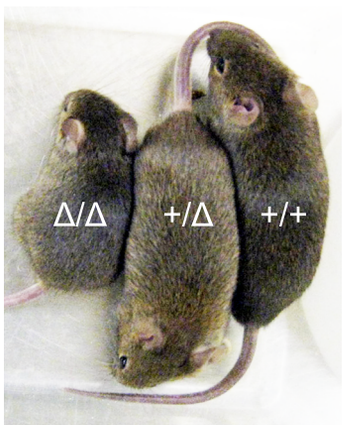

C

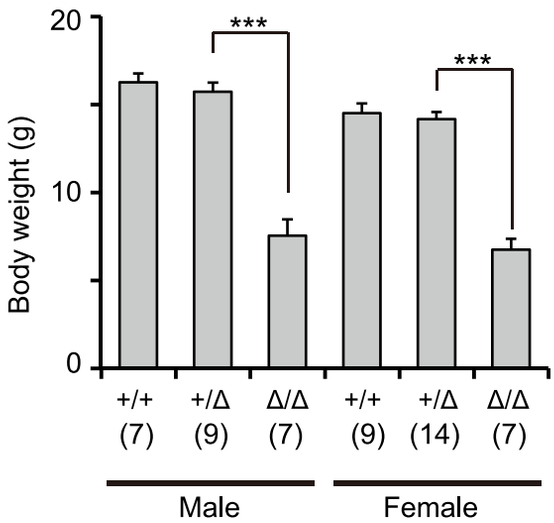

D

Jmjd1a :	+/+			+/Δ			Δ/Δ			
Jmjd1b :	+/+	+/Δ	Δ/Δ	+/+	+/Δ	Δ/Δ	+/+	+/Δ	Δ/Δ	Total
	10	23	10	16	36	4*	8	2*	0	109
Expected	6	12	6	12	25	12	6	12	6	

*All animals were stillborn.

Figure S2. Phenotypic Analysis of *Jmjd1b*-Deficient Mouse and *Jmjd1a*/*Jmjd1b*-Double Deficient Mouse, Related to Figure 1.

(A) *Jmjd1b*$^{+/\Delta}$ males and *Jmjd1b*$^{+/\Delta}$ females were crossed, and the resultant offspring were genotyped. The percentage of animals with the indicated genotypes is shown in the bar graph. *Jmjd1b*$^{\Delta/\Delta}$ mice were born at nearly the expected Mendelian ratio (P0), but most of them died within a week after birth (P7). The numbers of examined mice are shown in parenthesis. (B) Appearance of 6-week old littermate mice of *Jmjd1b* mutant mice. (C) The body weight of *Jmjd1b* mutant mice at 4-month-old age. The numbers of mice examined are shown in parenthesis. Data are presented as mean ± SD. ***P<0.001 (Student's test) (D) Genotype of newborn pups by mating *Jmjd1a*$^{+/\Delta}$; *Jmjd1b*$^{+/\Delta}$ males and females.

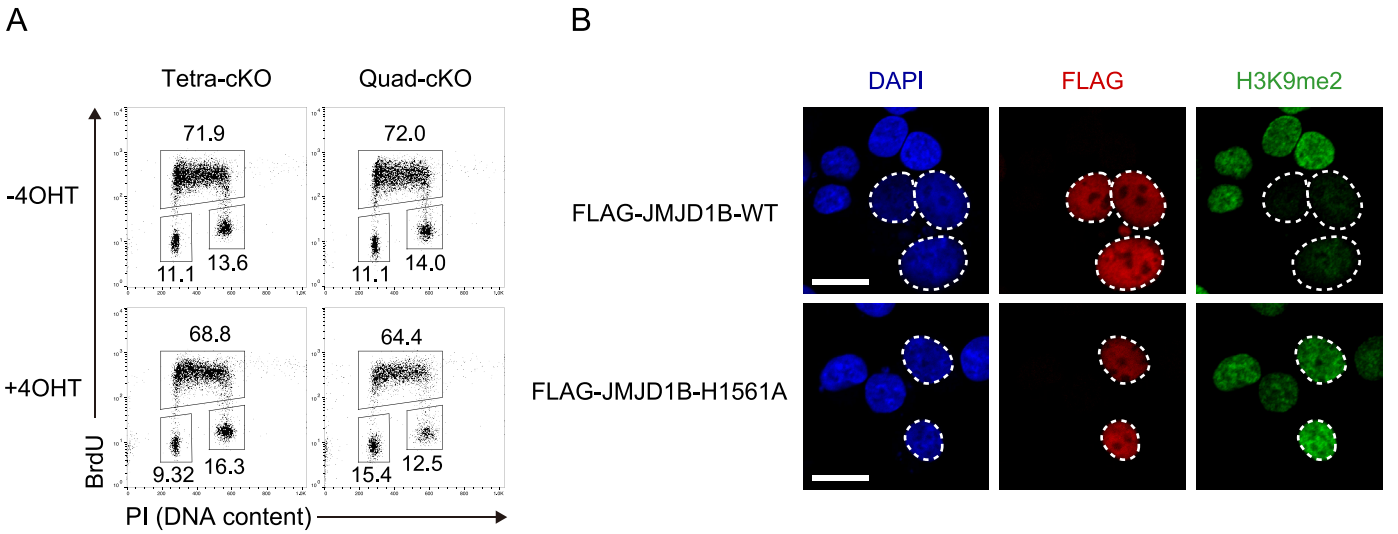

Figure S3. Phenotypic Analysis of JMJD1A/JMJD1B-Depleted ES cells, Related to Figure 2.
(A) Cell cycle analysis was conducted using 4OHT-treated Quad-cKO cells by measuring bromodeoxyuridine (BrdU) incorporation and the DNA contents. 4OHT treatment did not appear to have a profound effect on cell cycle progression in both Quad-cKO and Tetra-cKO cell lines. (B) Expression vectors for FLAG-tagged wild-type JMJD1B (upper) and mutant JMJD1B with H1561A mutation (bottom) were introduced into HEK293T cells. 2 days after introduction, cells were co-stained with anti-FLAG antibody (red) and anti-H3K9me2 antibody (green). Nuclei were counterstained with DAPI (blue). Scale bars, 20μm.

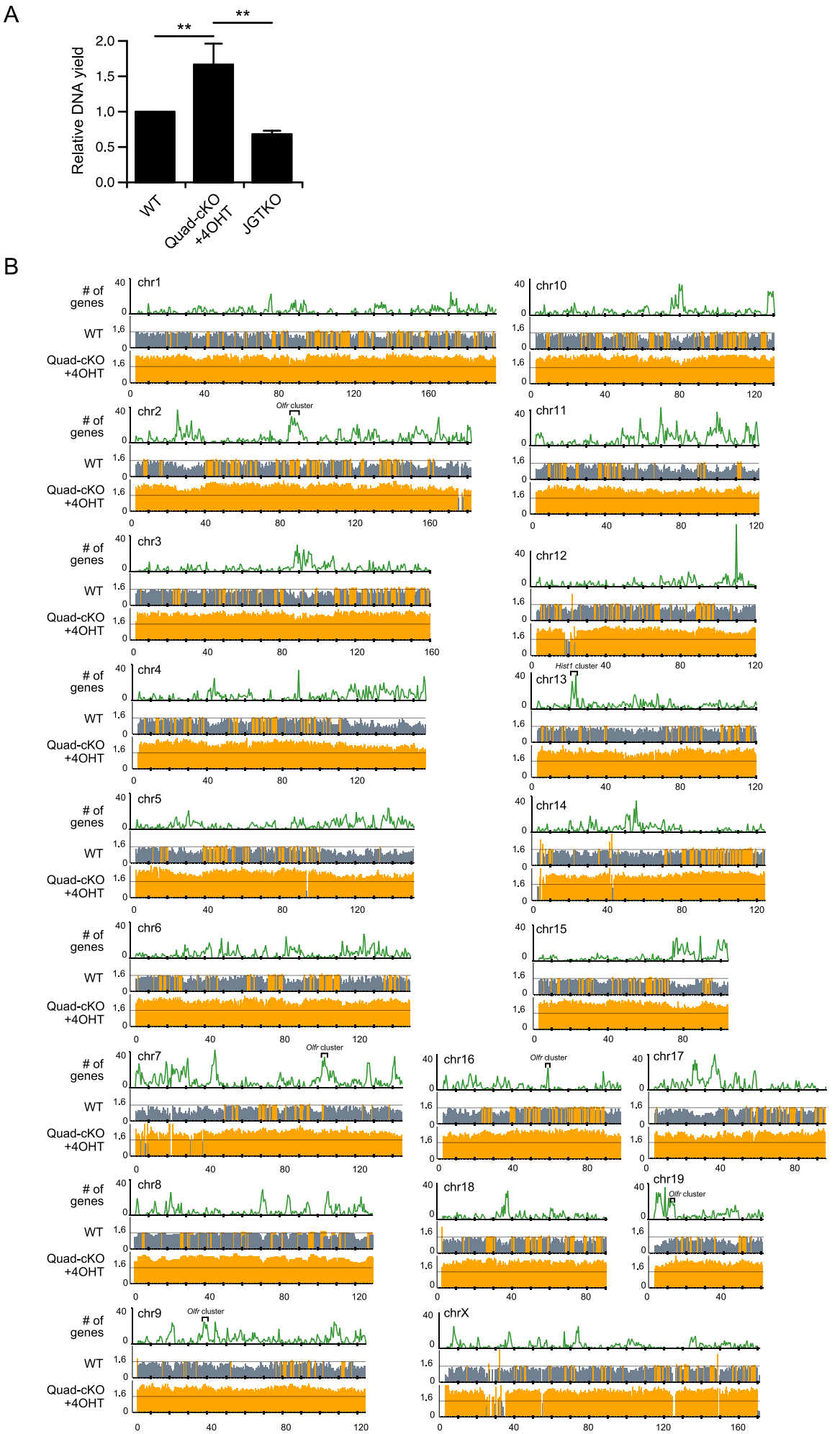
A
Relative DNA yield
2.0
1.5
1.0
0.5
0.0
**
**
WT
Quad-cKO +4OHT
JGTKO
B
# of genes
WT
Quad-cKO +4OHT
chr1
chr2
chr3
chr4
chr5
chr6
chr7
chr8
chr9
chr10
chr11
chr12
chr13
chr14
chr15
chr16
chr17
chr18
chr19
chrX
Olfr cluster
Hist1 cluster

Figure S4. ChIP Analysis of JMJD1A/JMJD1B-Depleted Cells with Anti-H3K9me2 Antibody, Related to Figure 4.

(A) Mononucleosomes were prepared from 2×10^5 ES cells of the indicated genotypes and subjected to native ChIP analysis with anti-H3K9me2 antibody. DNA was purified from immunеprecipitated chromatin and then subjected to quantification. DNA collected form wild-type cells was assumed as 1 for data normalization. Data are presented as mean ± SD (n=3 independent experiments). $^{**}P < 0.01$ (One-way ANOVA and Tukey HSD test). (B) Distribution profiles of H3K9me2 in chromosomes. The upper panel shows the number (#) of mm10 refseq genes smoothed with a 500 kb width. The middle and lower panels represent the ratios of normalized read density between ChIP and whole cell lysate (Input) samples (ChIP/Input) in wild-type (WT) and JMJD1A/JMJD1B-depleted cells (Quad-cKO+4OHT), respectively. The ratio of ChIP/Input > 1.6 are shown in orange. Several gene clusters, which had escaped from JMJD1A/JMJD1B-mediated H3K9 demethylation, are seen on the top panels.

A

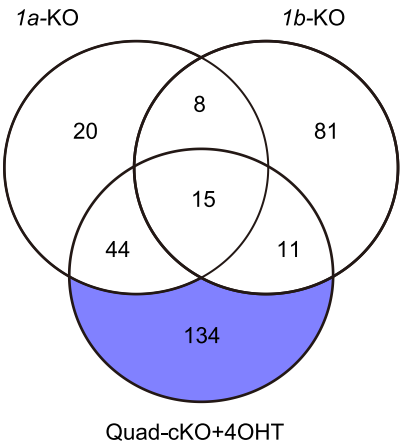

B

GO	Term	*p*-value
GO:0006730	one-carbon metabolic process	8.25×10^{-4}
GO:0030968	endoplasmic reticulum unfolded protein response	2.95×10^{-3}
GO:0007566	embryo implantation	5.54×10^{-3}
GO:0008152	metabolic process	6.58×10^{-3}
GO:0008652	cellular amino acid biosynthetic process	9.69×10^{-3}

C

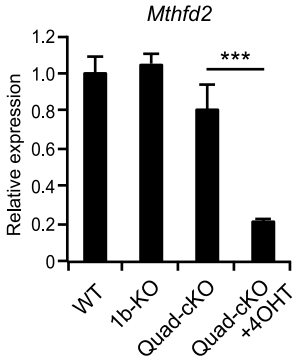

D

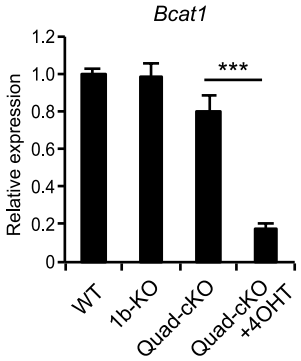

E

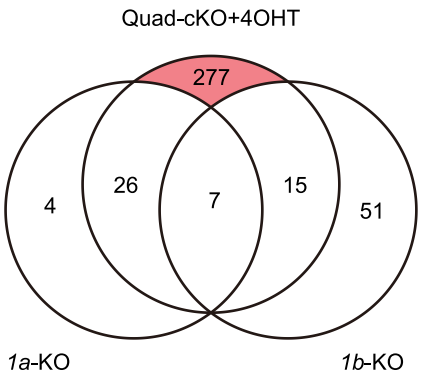

F

GO	Term	*p*-value
GO:0007286	spermatid development	7.47×10^{-11}
GO:0035458	cellular response to interferon-beta	1.27×10^{-6}
GO:0045596	negative regulation of cell differentiation	1.76×10^{-4}
GO:0008284	positive regulation of cell proliferation	5.16×10^{-4}
GO:0060333	interferon-gamma-mediated signaling pathway	1.10×10^{-3}
GO:0043066	negative regulation of apoptotic process	2.16×10^{-3}
GO:0086073	bundle of His cell-Purkinje myocyte adhesion involved in cell communication	2.71×10^{-3}
GO:0010833	telomere maintenance via telomere lengthening	4.97×10^{-3}
GO:0098911	regulation of ventricular cardiac muscle cell action potential	6.33×10^{-3}
GO:0044406	adhesion of symbiont to host	6.33×10^{-3}
GO:0086091	regulation of heart rate by cardiac conduction	6.48×10^{-3}
GO:0005975	carbohydrate metabolic process	7.69×10^{-3}
GO:0042832	defense response to protozoan	7.87×10^{-3}
GO:0007569	cell aging	7.87×10^{-3}
GO:0007129	synapsis	7.87×10^{-3}

Figure S5. Gene Ontology Analysis for Genes Regulated by JMJD1A and JMJD1B, Related to Figure 5.
(A) The number of genes whose expression was reduced by the depletion of JMJD1A, JMJD1B, or both is shown. Venn diagram indicates down-regulation of 134 genes in JMJD1A/JMJD1B-depleted cells. (B) Significantly enriched GO terms ($p < 0.01$) in 134 down-regulated genes. (C, D) RT-qPCR analysis of *Mthfd2* (methylenetetrahydrofolate dehydrogenase 2) and *Bcat1* (branched-chain amino acid transaminase 1). Both these genes were selected from the group of 134 down-regulated genes in JMJD1A/JMJD1B-depleted cells. MTHFD2 and BCAT1 are the key enzymes for one-carbon metabolism and amino acid catabolism, respectively. The expression levels of *Mthfd2* (C) and *Bcat1* (D) were drastically reduced due to the double mutation, but not single mutation, indicating that JMJD1A and JMJD1B redundantly activate these genes. Data are presented as mean ± SD (n=3 independent experiments). ***$P < 0.001$ (Student's *t* test). (E) The number of genes whose expression was up-regulated by the depletion of JMJD1A, JMJD1B, or both is summarized. Venn diagram indicates 277 genes up-regulated genes in JMJD1A/JMJD1B-depleted cells. (F) Significantly enriched GO terms ($p < 0.01$) in the 277 genes up-regulated by JMJD1A and JMJD1B in a redundant manner.

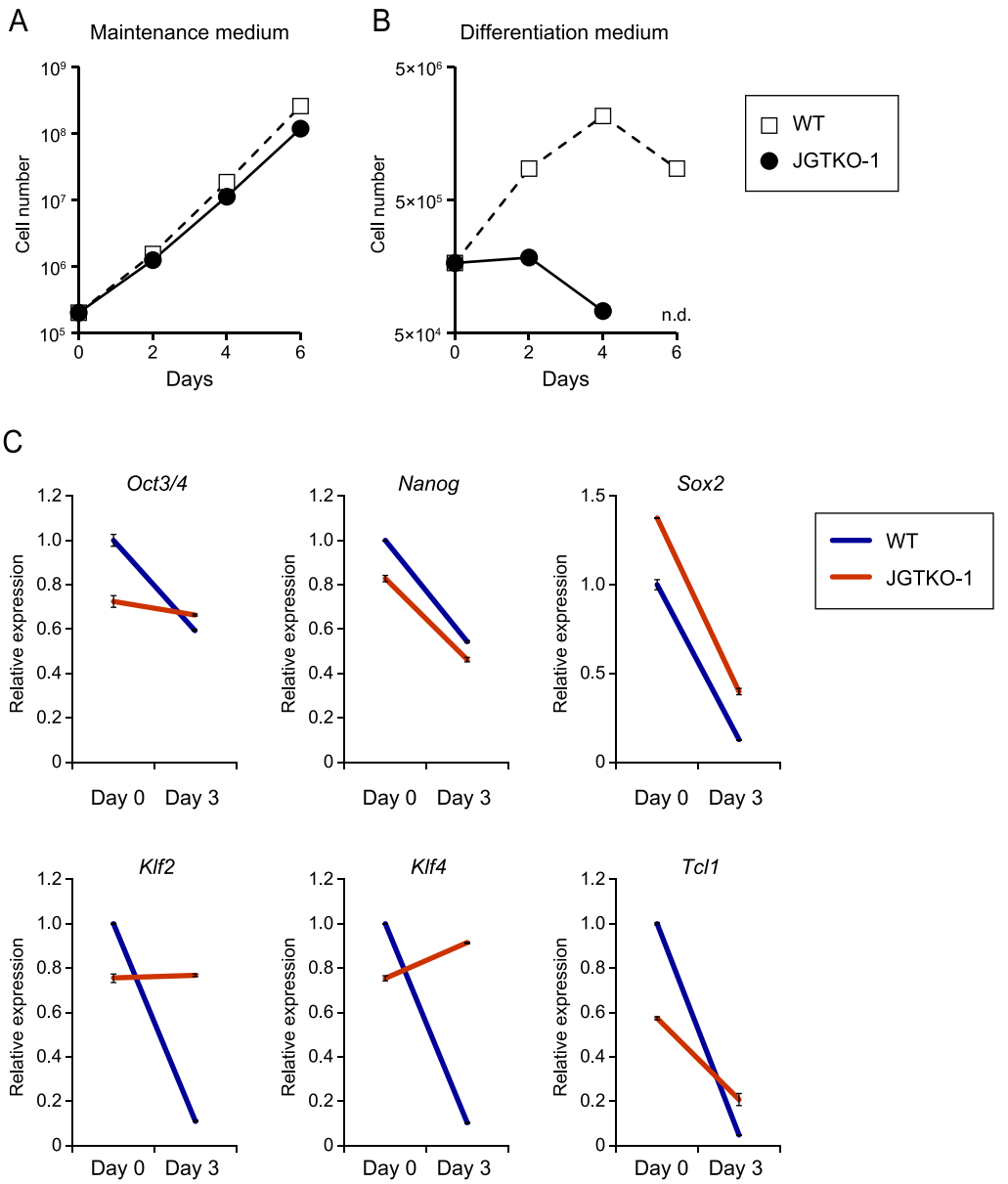

Figure S6. JMJD1A/JMJD1B- And G9A-Mediated H3K9 Methylation Tuning Is Important for ES Cell Differentiation, Related to Figure 6 and 7.

(A, B) Growth potential of JMJD1A/JMJD1B- and G9A-triple knock-out cells. JMJD1A/JMJD1B/G9A-triple deficient JGTKO-1 line was cultured in the maintenance medium (A) or in a differentiating medium without leukemia inhibitory factor (B; see Materials and Methods). (C) Perturbed transcriptional regulation of pluripotency-associated genes in JMJD1A/JMJD1B/G9A triple-deficient JGTKO-1 line under differentiating condition. Cells were cultured in the differentiation medium for 3 days, and mRNA expression of the indicated genes was analyzed using RT-qPCR. Values of gene expression in wild-type cells were considered as 1 for data normalization. Representative data are presented from n=3 independent experiments. Error bars indicate mean ± SD derived from technical replicates..

Table S1. Primer List Used in This Study

Primer name	Application	Sequence (5'->3')
2B-65420F	Probe synthesis for Southern blot analysis	AGGAAGCTGGCAGACCAGTA
2B-65900R		CGTTCTTCACCGACTTCCTC
Gapdh RT-PCR F	RT-qPCR	ATGAATACGGCTACAGCAACAGG
Gapdh RT-PCR R		CTCTTGCTCAGTGTCCTTGCTG
Jmjd1b 62315F	RT-qPCR	GGAGATGCTGATGAGGTGACCAAGC
Jmjd1b 62415R		GGATCTTCTCTGCATCCTTCGCTGC
2B-60841F	Detection of *Jmjd1b*+ and *Jmjd1b*! alleles	GCACCAAGCACTGCCACGGAGCTGA
2B-63090R		GATTAAAGGCTTGCACTACTAGACTCACTG
2B-61290R		ACCAGGTGCCGCTACATGAAGCTGG
TSGA-G2150F	Detection of *Jmjd1a*+ and *Jmjd1a*! alleles	CATACTGGTCTCCAGGAGCCAGAGG
TSGA-G1475R		GAACTGCACCATTAGCTGTCACTTCC
TSGA-G6540F		TCAGACAGTCCTGGGATCAGACACAC
Oct4-F	RT-qPCR	TGAGAACCGTGTGAGGTGGAGTCTG
Oct4-R		AAGCTGATTGGCGATGTGAGTGATC
Ccnd1-F	RT-qPCR	CGAAGAGGAGGTCTTCCCGCTGGCC
Ccnd1-R		CCCAGCAGCTGCAGGCGGCTCTTCT
Nnog-F	RT-qPCR	TTTGGAGGTGAATTTGGAAGC
Nanog-R		TCACCTGGTGGAGTCACAGAG
Sox2-F	RT-qPCR	CTTGCTGGGTTTTGATTCTGC
Sox2-R		AAGACCACGAAAACGGTCTTG
Klf2-F	RT-qPCR	CCCCAGGAAAGAAGACAGGAG
Klf2-R		AGGCATTTCTCACAAGGCATC
Klf4-F	RT-qPCR	GACCAGGATTCCCTTGAATTG
Klf4-R		ACCAAGCACCATCATTTAGGC
Tcl1-F	RT-qPCR	TGGCCTCACTAGAACAAGAGG
Tcl1-R		CTCGGTCAAGGATGGAAGC
Brachyury-F	RT-qPCR	AAGGACAGAGAGACGGCTGTG
Brachyury-R		AAAGTAGGACAGGGGGTGGAC
Fgf5-F	RT-qPCR	ATGAGTGCATCTGCTCTGCTC
Fgf5-R		CGTCTGTGGTTTCTGTTGAGG
Gata4-F	RT-qPCR	CTCCAGCCTGAACATCTACCC
Gata4-R		TGTGTGTGAAGGGGTGAAAAG
Mthfd2 #2 Fwd	RT-qPCR	AGAACCTCACCAGGATGCCCATCAG
Mthfd2 #2 Rev		TTCAGCATCCACTCTCGGTGTGAGG
Bcat1-e1 F	RT-qPCR	TGAGTTTAAGGTATGTGAGAGACAC
Bcat1-e1 R		CTGTCCCTGAGCCGAACATCTCCTT
Oct4-p-F	ChIP-qPCR	ATGGTGTAGAGCCTCTAAACTCTGG
Oct4-p-R		GTGAACCCAGTATTTCAGCCCATGT
Ccnd1-p1-F	ChIP-qPCR	CATTGCTTAGAAATCCCAGCGTCCC
Ccnd1-p1-R		CTCGTCTGGCATCTTCGGGTGTTAC

Supplemental Experimental Procedures

Antibodies

The poly histidine tag-fused polypeptide corresponding to amino acids 518K to 647H of JMJD1B (NP 001074725) was bacterially expressed, purified, and then used to immunize a rabbit. Rabbit polyclonal antibodies used against JMJD1A have been described previously (Tachibana et al., 2007). The other antibodies used in this study were anti-FLAG (M2, Sigma), anti-OCT3/4 (Abcam, ab19857), anti-β-actin (Wako, 013-24553), anti-G9A (Perseus Proteomics, #8620), anti-tubulin (Merck Millipore, CP06), anti-BrdU (BD Biosciences, 347580) and a panel of mouse antibodies against H3K9me1 (clone 2F7a), H3K9me2 (clone 6D11), and H3K9me3 (clone 2F3) (Kimura et al., 2008). For ChIP analysis, anti-H3K9me2 (Abcam, Ab1220) was used.

Immunofluorescence analysis

The embryos were fixed in 4% paraformaldehyde for 2 h at 4°C. For immunohistological analysis, the embryos were embedded in paraffin and cut into 4-μm-thick sections using a standard protocol. The sections were deparaffinized, rehydrated, and heated at 105°C for 5 min in10 mM citric acid buffer (pH 6.0). For whole-mount immunostaining, fixed embryos were permeabilized with PBS containing 0.5% Triton-X100 and 1% BSA for 20 min at RT. For immunocytochemistry, ES cells were cultured in slide chambers (ibidi) in the presence of 4OHT (800 nM) for 4 days. The cells were fixed in 2% PFA for 15 min, followed by permeabilization with 0.2% Triton-X100 for 30 min at RT.
For immunofluorescence staining, samples were blocked with TBS containing 2% skim milk and 0.1% Triton X-100 for 1 h, and then, incubated with the primary antibodies overnight at 4°C. This was followed by incubation with Alexa-conjugated secondary antibodies for 1 h and counterstaining with DAPI (1 μg/ml). The samples were mounted in Vectashield (Vector) and analyzed by confocal scanning microscopy (LSM700, Carl Zeiss). For whole-mount immunofluorescence analysis, Z-stack images (1 μm each) were collected and the maximum projections were processed using Zen 2011 imaging software (Carl Zeiss). Fluorescence intensity was measured using NIH ImageJ software.

Generation of *Jmjd1b*-deficient mice

The *Jmjd1b* knock-in targeting vector was constructed by the bacterial artificial chromosome (BAC) recombineering technique (Copeland et al., 2001) (Supplemental Fig. S1C), and then introduced into the ES cell line TT2. Homologous recombinant clones were identified by Southern blot analysis (Supplemental Fig. S1F). Chimeric males derived from two independent ES clones were used to generate F1 offspring bearing the mutant alleles, which were further crossed with *Pgk-2 Cre* transgenic mice (Ando et al., 2000), in order to generate the $Jmjd1b^{\Delta}$ allele. The resultant $Jmjd1b^{\Delta/+}$ females and males were crossed to generate *Jmjd1b*-deficient mice and embryos. All animal experiments were performed under the animal ethical guidelines of Tokushima University (experiment number 14108, approved by The Ethics Committee of Tokushima University for Animal Research) and Kyoto University (experiment number A12-6-2, approved by Animal Experimentation Committee of Kyoto University).

Generation of *Jmjd1b*-deficient ES cells

Jmjd1b-conditional targeting vector was constructed using the BAC recombineering technique (Supplemental Fig. S1D) and introduced into the $Jmjd1b^{\Delta/+}$ ES cell line 2b-11. Homologous recombination was confirmed by Southern blot analysis with the aforementioned probe. The homologous recombinant ES cell line YY90 (genotype: $Jmjd1b^{\Delta/2lox2FRT}$) was used for further evaluation. The

Jmjd1b-deficient ES cell lines, D23.6 and D4.1 (genotype: $Jmjd1b^{\Delta/1lox2FRT}$), were established from a pool of YY90 cells infected with Cre-expressing recombinant adenoviruses.

Generation of ES cells carrying the *Jmjd1a* knockout- and *Jmjd1b*-conditional knockout alleles

Jmjd1b conditional targeting vector was introduced into the *Jmjd1a*-deficient ES line 31-1 (Inagaki et al., 2009). The expression plasmid for MerCreMer was then introduced into the recombinant ES cell lines #117 and #131 (genotype: $Jmjd1a^{\Delta/\Delta}$; $Jmjd1b^{2lox1FRT/2lox2FRT}$).

Generation of ES cells lacking JMJD1A, JMJD1B, and G9A

G9a conditional targeting vector was introduced into the ES line #131. Homozygous mutants for the *G9a*-conditional knockout allele were successfully obtained when heterozygous mutants were cultured with 2.4 mg/ml G418 (3 of 40 clones). The plasmid for MerCreMer expression was introduced into the ES line 131-30-1 (genotype: $Jmjd1a^{\Delta/\Delta}$; $Jmjd1b^{2lox1FRT/2lox2FRT}$; $G9a^{2lox/2lox}$).

TUNEL assay

TdT-mediated UTP nick end labeling (TUNEL) was performed against the immunostained whole-mount embryos using the In Situ Cell Death Detection Kit (Roche) according to manufacturer's instructions. Images were collected and analyzed with the LSM700 microscope and Zen 2011 imaging software (Zeiss), respectively.

FACS analysis

ES cells were cultured in the presence of 4OHT (800 nM) for 2 or 4 days. For the cell death analysis, PI/annexin-V staining was performed using the MEBCYTO Apoptosis assay kit (MBL) according to the manufacturer's protocol. For the cell cycle analysis, deoxyuridine (BrdU) and PI staining was performed as described previously (Iwano et al., 2004) with some modifications. Briefly, ES cells were labeled with 20 μM BrdU for 30 min and fixed in 70% ethanol. The fixed cells were treated with 2 N HCl, washed in 1% BSA/PBS, and stained with anti-BrdU antibody. After washing, the cells were incubated with Alexa488-conjugated secondary antibody. Subsequently, the cells were incubated with RNase; PI (10 μg/ml) was added just before the analysis. The flow cytometric analysis was performed with a FACS Canto II flow cytometer (BD Biosciences).

ES cell culture

ES cells were maintained in Dulbecco's modified Eagle's medium, containing 10% knockout SR (Invitrogen), 1% fetal calf serum, and leukemia-inhibiting factor (10^3 U/ml). To delete the conditional allele of *Jmjd1b*, ES cells were cultured in the presence of 800 nM OHT. In the differentiation experiments of ES cells, cells were cultured in Dulbecco's modified Eagle's medium containing 10% fetal calf serum without leukemia-inhibiting factor.

Genotyping

Genotyping of the *Jmjd1a*-deficient and *Jmjd1b*-deficient mice/embryos was performed by PCR using the primers described in Supplemental Table S1.

Immunoblot analysis

Whole lysates of ES cells were fractionated by SDS electrophoresis and transferred to nitrocellulose membranes. The membranes were visualized with an enhanced chemiluminescence (ECL) kit (Perkin Elmer). The band intensities were quantified using the ImageJ software (National Institutes of Health).

ChIP analysis

Native ChIP of H3K9me2 was performed following a protocol described previously (Tachibana et al., 2008) with a slight modification. Briefly, 2 x 10^5 cells were suspended in 25 µl of 0.3 M sucrose-containing buffer 1 (60 mM KCl, 15 mM NaCl, 5 mM MgCl2, 0.1 mM EGTA, 0.5 mM DTT, 15 mM Tris-HCl pH 7.5, and protease inhibitor cocktail). The cells were then lysed following the addition of 0.3 M sucrose-containing buffer 1 (25 µl) with 0.8% NP40 on ice for 10 min; 1.2 M sucrose-containing buffer 1 (400 µl) was added and the chromatin was collected as pellets by centrifugation. The pellets were digested with micrococcal nuclease (0.05 U, Takara) in 10 µl of digestion buffer (0.32 M sucrose, 4 mM $MgCl_2$, 1 mM $CaCl_2$, 50 mM Tris-HCl pH 7.5) by vortexing at 37°C for 15 min; digestion was stopped with EDTA. The supernatant was obtained by centrifugation and incubated with anti-H3K9me2-conjugated magnetic beads (Dynabeads Protein G, Invitrogen) in 50 µl of incubation buffer (50 mM NaCl, 5 mM EDTA, 0.1% NP40, 20 mM Tris-HCl pH 7.5) at 4°C for 6 h. Then, DNA was extracted from the immune complex according to the standard protocol and quantified using Qubit ds DNA HS Assay Kit (Thermo Fisher Scientific), and then analyzed by real-time PCR. For ChIP of JMJD1A and FLAG-tagged JMJD1B, cross-link ChIP was performed following a protocol described previously (Kuroki et al., 2017).

ChIP-Seq analysis

DNA from input and Native ChIP fractions of H3K9me2 was processed and sequenced using the Illumina HiSeq-2500 system according to the manufacturer's instructions. In brief, the DNA was sheared to a mean size of ~150 bp by ultrasonication (Covaris), end-repaired, ligated to sequencing adapters, amplified, size-selected, and sequenced to generate single-end reads. Sequence reads were mapped to mouse mm10 genome using Bowtie2 (v 2.1.0) after trimming the first base from 5' end of reads (-5 1 option). Only uniquely mapped and non-redundant reads were used for further analysis. The mapped reads were processed and visualized using DROMPA (v 3.2.6) (Nakato et al., 2013). To compare WT and Quad-cKO and JGTKO ChIP-seq data, ChIP and input reads were normalized to the concentration of ChIPed DNA after normalization for read numbers (Supplemental Fig. S4 and S6). The processed reads were visualized using the GV (with -binsize 500000 option; to show the ratio of normalized read density between ChIP and input samples) and PC_ENRICH (with -binsize 5000 option; to show the normalized read density of ChIP and the corresponding input samples) commands in DROMPA. Down- and up-regulated genes were defined as genes having log2 fold change < -1 or > 1, respectively, in Quad-cKO + 4OHT versus WT. Plotting of averaged reads around gene bodies was performed using the PROFILE command in DROMPA based on the following parameters: -ptype 3 -stype 1 -binsize 5000.
ChIP-seq data from this study have been submitted to DDBJ Read Archive database (http://trace.ddbj.nig.ac.jp/dra/index_e.shtml) under accession number "DRA006496".

Microarray analysis

Total RNA was purified from ES cells with an RNeasy mini kit (Qiagen). DNA microarray analysis was performed according to the manufacturer's protocol. In brief, biotinylated cRNA was synthesized from 200 ng of total RNA and hybridized to an Affymetrix Mouse Genome 430 2.0 array. Affymetrix GeneChip Command Console software was used to reduce the array image to the intensity of each probe (CEL files). All microarray data are MIAME compliant and have been deposited in a MIAME-compliant database, the National Center for Biotechnology Information (NCBI) Gene Expression Omnibus

(http://www.ncbi.nlm.nih.gov/geo/, GEO Series accession number GSE98761), as detailed on the FGED Society website (http://fged.org/projects/miame/).
The CEL files were quantified with the factor analysis for robust microarray summarization (FARMS) (Hochreiter et al., 2006) using R (http://www.r-project) and Bioconductor (http://www.bioconductor.org/) (Gentleman et al., 2004). Hierarchical clustering was performed using the pvclust function (Suzuki and Shimodaira, 2006). The annotation file for Mouse Genome 430 2.0 Array was downloaded from the Affymetrix website (October 23, 2013, Mouse430_2.na34.annot.csv).

Supplemental Reference

Ando, H., Haruna, Y., Miyazaki, J., Okabe, M., and Nakanishi, Y. (2000). Spermatocyte-specific gene excision by targeted expression of Cre recombinase. Biochemical and biophysical research communications *272*, 125-128.

Copeland, N.G., Jenkins, N.A., and Court, D.L. (2001). Recombineering: a powerful new tool for mouse functional genomics. Nature reviews Genetics *2*, 769-779.

Gentleman, R.C., Carey, V.J., Bates, D.M., Bolstad, B., Dettling, M., Dudoit, S., Ellis, B., Gautier, L., Ge, Y., Gentry, J.*, et al.* (2004). Bioconductor: open software development for computational biology and bioinformatics. Genome Biol *5*, R80.

Hochreiter, S., Clevert, D.A., and Obermayer, K. (2006). A new summarization method for Affymetrix probe level data. Bioinformatics *22*, 943-949.

Inagaki, T., Tachibana, M., Magoori, K., Kudo, H., Tanaka, T., Okamura, M., Naito, M., Kodama, T., Shinkai, Y., and Sakai, J. (2009). Obesity and metabolic syndrome in histone demethylase JHDM2a-deficient mice. Genes Cells *14*, 991-1001.

Iwano, T., Tachibana, M., Reth, M., and Shinkai, Y. (2004). Importance of TRF1 for functional telomere structure. J Biol Chem *279*, 1442-1448.

Kimura, H., Hayashi-Takanaka, Y., Goto, Y., Takizawa, N., and Nozaki, N. (2008). The organization of histone H3 modifications as revealed by a panel of specific monoclonal antibodies. Cell Struct Funct *33*, 61-73.

Kuroki, S., Okashita, N., Baba, S., Maeda, R., Miyawaki, S., Yano, M., Yamaguchi, M., Kitano, S., Miyachi, H., Itoh, A.*, et al.* (2017). Rescuing the aberrant sex development of H3K9 demethylase Jmjd1a-deficient mice by modulating H3K9 methylation balance. PLoS Genet *13*, e1007034.

Nakato, R., Itoh, T., and Shirahige, K. (2013). DROMPA: easy-to-handle peak calling and visualization software for the computational analysis and validation of ChIP-seq data. Genes Cells *18*, 589-601.

Suzuki, R., and Shimodaira, H. (2006). Pvclust: an R package for assessing the uncertainty in hierarchical clustering. Bioinformatics *22*, 1540-1542.

Tachibana, M., Matsumura, Y., Fukuda, M., Kimura, H., and Shinkai, Y. (2008). G9a/GLP complexes independently mediate H3K9 and DNA methylation to silence transcription. The EMBO journal *27*, 2681-2690.

Tachibana, M., Nozaki, M., Takeda, N., and Shinkai, Y. (2007). Functional dynamics of H3K9 methylation during meiotic prophase progression. The EMBO journal *26*, 3346-3359.